Effect of loading frequency on deformations at the bone-implant interface

Effect of loading frequency on deformations at the bone-implant interface

Shuqiao Xie[1], Krishnagoud Manda[1,2], Pankaj Pankaj[1*]

[1] School of Engineering, Institute for Bioengineering, The University of Edinburgh, Alrick Building, The King's Buildings, Edinburgh EH9 3BF, UK

[2] School of Mechanical and Aerospace Engineering, Queen's University Belfast, Stranmillis Road, Belfast BT9 5AH, UK

Abstract

This study considers time-dependent behaviour of bone in the context of loosening of metal implants, which is one of the typical complications of joint replacement and fracture fixation surgeries. We employed viscoelastic properties developed from our previous experimental studies for trabecular bone in a representative bone-implant construct, which was subjected to cyclic loading at varying loading frequencies. We found that the separation between the bone and the implant is a function of loading frequency and increases with number of loading cycles applied. Our analysis shows that at the start of cyclic loading a higher frequency results in a lower displacement response of bone at the bone-implant interface; however after the bone-implant system has been subjected to a large number of cycles (>500 cycles in this study), higher interfacial displacements are observed at higher loading frequencies. In other words, higher loading frequencies will not result in bone-implant separation if limited number of cycles are applied. In all cases interfacial displacements increase as bone volume ratio decreases. This simple approach can be used to evaluate the mechanical environment in bone-implant systems due to cyclic loading which commonly used time-independent models are unable to simulate. The approach can also be used to evaluate implant loosening due to cyclic loading.

Keywords: bone volume ratio; cyclic loading; displacement accumulation; viscoelastic; time-dependent behaviour

Introduction

Many forms of joint replacement (e.g. hip[1], knee[2]) and fracture-fixation treatments (e.g. external fixators[3], locking plates[4,5]) employ bone-implant constructs which experience cyclic loading due to normal physiological activities. Aseptic loosening is the failure of the bond between bone and implant in the absence of infection. Aseptic loosening is recognised as the most common cause of revision in major arthroplasties[1,2,6]. It has been suggested that high strains in the bone at the bone-implant/screw interface can initiate

loosening[7] which can result in infection and further loosening.[8–10] Micromotion at the bone-implant interface is an important parameter that determines the primary stability of the implant and is often caused by deformation of bone.[6] A common pattern of migration, initial rapid phase followed by a slower continuous phase, has suggested that the early loosening of implant is a mechanical phenomenon or at least mechanically triggered [11]. Experimental investigations have shown that the bone-implant interface micromotion is a function of the number of loading cycles for a range of implants used for total hip replacement, femoral fracture fixation, spinal fracture fixation and radius fracture fixation.[12–15]

Trabecular bone is recognised as time-dependent material.[16–18] The displacement (or strain) response of bone to cyclic loads is a function of cycles (i.e. bone's cyclic loading history)[19–21] and the loading frequency[22]. Almost all previous studies that considered modelling of bone-implant systems assumed bone to have a time-independent mechanical response (i.e. it deforms instantaneously on load application)[4,9,23,24], though in some studies bone was assumed to be elastic while others modelled it as nonlinear [3,25]. To the best of authors' knowledge, there are only two studies that have employed time-dependent behaviour of bone in computational simulation. Shultz et al. reported that bone's viscoelastic behaviour, namely stress relaxation, has an asymptotic effect on stem contact pressure for press-fit femoral stems, which reduces stem pull-out load. [26] Xie et al. employed nonlinear-viscoelastic and nonlinear viscoelastic-viscoplastic material for a bone-implant system and showed that interfacial deformations in the bone increased with cycle numbers. [27] However, the effect of loading frequency on bone-implant interface mechanics has not been previously considered.

This study uses the experimentally developed bone volume ratio (BV/TV)-based linear viscoelastic constitutive model [18] to evaluate the mechanical environment at the interface of an idealised bone-implant construct subjected to cyclic loading at different frequencies. The aims of this study were to examine the relative deformation between the bone and the implant when bone is modelled as a viscoelastic material. The effect of BV/TV, loading frequency and number of cycles on interfacial deformations is evaluated.

Material and Methods

An idealised system, two-dimensional plane strain construct, with a representative implant and surrounding bone as shown in Fig. 1a was employed. Bone-screw systems used in unilateral fixators and locking plates motivated the choice this idealised system. It is, however, clear that this is a simplification of reality as the screw would be cylindrical whereas a plane strain representation implies a plate-like implant. However, since the plane-strain assumption provides confinement in the out-of-plane direction, it is expected to provide representative results in the plane of the model. The model was kept simple to maintain transparency of the results i.e. to ensure that the response is due to the assignment of viscoelastic properties to trabecular bone subjected to cyclic loading at varying frequencies without adding complications associated with the geometry.

Perfect fit between the implant and the bone was assumed along the length of the implant while a small gap was included between the implant end and the bone to avoid influence of any end shape effects and maintain simplicity. The implant was assumed to be unicortical and a 1mm thick cortex was included in the model as shown in Fig. 1a.

The geometry was meshed using 4930 6-noded modified plain strain elements (CPE6M) in Abaqus 6.12 (Simulia, Providence, RI, USA). Mesh convergence studies were performed and they show that further mesh refinement resulted in an increase of maximum displacement of bone by less than 0.3%.

The implant and cortical bone were assumed to be homogeneous, isotropic and time-independent materials, with Young's modulus of 180 GPa and 20.7 GPa, respectively[23]. BV/TV-based viscoelastic material properties were employed to define the time-dependent properties of trabecular bone in which the relaxation modulus function, $E(t)$, is given by [18]

$$E(t) = B\phi^p + B\left[\sum_{i=1}^{3} \tilde{E}_i \exp\left(-\frac{t}{\tilde{\rho}_i}\right)\phi^{p_t}\right] \quad (1)$$

where ϕ is the BV/TV of trabecular bone, t is time and B, p, p_t, $\tilde{E}_i$ and $\tilde{\rho}_i$ are constant material coefficients evaluated as given in Table 1[18]. Consequently, ϕ is the only variable in the evaluation of relaxation modulus function. Three BV/TV values were selected: 15%, 25% and 35% as they represent commonly found low, medium and high bone volume fractions. Poisson's ratio of ν=0.3 [4,23] was applied to all the materials.

A standard Coulomb friction coefficient of 0.3 [23] was employed based on some of the recent studies[4,23], with surface-to-surface frictional contact assumed at the bone-implant interface. Translation degree of freedoms at all edges of bone section were constrained except at the edge with screw hole, as shown in Fig. 1a.

A 300 N concentrated triangular cyclic loading (Fig 1b) was applied at the right end of the implant over a thickness of 3.25 mm (Fig. 1a) with designated loading

frequencies for 2000 cycles. One complete cycle includes a ramp loading and unloading. Seven loading frequencies, f, from 0.1 Hz to 10 Hz were investigated (Fig. 1c), which cover the physiological frequency range of normal human activities from slow walking to running.[28] There were 21 models included in this study: 3 BV/TV material models at 7 different loading frequencies.

Results

Eight selected cycles were considered for this comparative study, cycle 1, 5, 10, 100, 500, 1000, 1500 and 2000 denoted as C1, C5, C10, C100, C500, C1000, C1500 and C2000, respectively. The maximum displacements within trabecular bone were extracted and plotted against loading frequencies for the above 8 cycles as shown in Fig. 2 for both loaded (when the load is at its peak) and unloaded (when the construct is completely unloaded) phases with varying BV/TV. The displacement contours for BV/TV = 15% at the unloaded phase are shown in Fig. 3 for the above 8 selected cycles.

We first consider the displacement at the loaded phase. Maximum displacement of trabecular bone at the loaded phase, for all BV/TV values considered, plotted against loading frequencies at selected cycles is shown in Fig. 2a, 2c and 2e. It is apparent that at C1 for BV/TV = 15% (Fig. 2a), f=0.1Hz has the largest displacement compared to other loading frequencies. These plots also show that the maximum displacement reduces with increase in frequency in the initial loading cycles (e.g. Cycle 1 response in Fig. 2a reduces with frequency). However, higher maximum displacement is observed at higher loading frequencies after a number of loading cycles (e.g. >500 cycles). Rapid increase in displacement with increased cycle numbers was observed for higher loading frequency

cases. At the end of C2000, the maximum displacement for f=10Hz is much higher than maximum displacement observed for f=0.1Hz.

These observations were also found to be true for the other two samples (BV/TV = 25% and 35%) considered in this investigation, and the results are shown in Fig. 2c and 2e for BV/TV = 25% and 35% respectively. Additionally, if the bone-implant construct is loaded at the same frequency for the same number of cycles, then, as expected, higher maximum displacement is obtained with a lower BV/TV sample (Fig. 3a, 3c and 3e).

We now consider the displacements upon unloaded phase. The maximum displacements of trabecular bone in the unloaded phase plotted against loading frequencies at 8 selected cycles are shown in Fig. 2b, 2d and 2f for BV/TV = 15%, 25% and 35%, respectively. As would be expected, majority of the displacements recover immediately upon unloading in the initial cycles as shown in Fig. 2. It is clear that the loading frequencies significantly affect the maximum displacement experienced by trabecular bone. For BV/TV = 15%, at lower cycles (e.g. below say C500), the higher displacement was observed at low loading frequencies (Fig. 2b). With further increase in cycle numbers, rapid increase in maximum displacement with increased cycle numbers can be observed for higher loading frequencies. In other words, the displacement that remained at unloaded time points accumulated much faster at high loading frequencies, and this was found to be true for all the BV/TV samples examined in this study (Fig. 2b, 2d and 2f). At C2000, f=10Hz had the largest maximum displacement, and it was more than four times of maximum displacement observed for f=0.1Hz (Fig. 2).

Similar to the loaded phase, the observed displacement at the unloaded phase was related to BV/TV of bone; for trabecular bone with higher BV/TV, lower displacement was observed, i.e. for the bone-implant construct loaded at the same frequency for the same number of cycles, a much smaller maximum displacement was observed when trabecular bone had higher BV/TV (Fig. 3b, 3d and 3f).

The observations from the peak displacement within trabecular bone are confirmed by the contour plot which shows the displacement distribution for the entire section of the bone. Figure 3 shows the contour plots of the bone when the bone-implant system upon unloaded phase. At lower cycles, lower loading frequencies resulted in larger displacement of bone at the interface compared to the higher loading frequencies (e.g. at C1, f=0.1Hz case results in larger displacement of bone compared to f=10Hz case). The displacement upon unloading accumulated significantly with increasing cycle numbers, which was true for all the loading frequencies. With increasing loading cycles, relatively larger displacement was observed when the bone-implant construct was loaded at higher loading frequencies (e.g. at C2000, f=10Hz case has relatively larger displacement compared to f=0.1Hz case). It essentially means that the displacement in the bone is accumulated much faster if the bone-implant constructed is loaded at higher loading frequencies.

Discussion

This study shows that the interfacial displacements in trabecular bone due to cyclic loading applied to the implant in a bone-implant construct are a function of loading cycles and loading frequencies. At the beginning of cyclic loading, lower loading

frequencies result in higher displacement in trabecular bone for both loaded and unloaded phases; while with increased cycle numbers, higher displacements are observed at higher loading frequencies. In all cases displacements increase as BV/TV decreases. It is reasonable to assume that there are two linked mechanisms at play: effect of time-dependent material response and dynamic effect due to frequency of loading.

In the initial cycles, higher frequency resulted in lower displacement response for both loaded and unloaded phases. This shows that the viscoelastic model used is able to capture the phenomenon observed in previous studies: higher strain rates result in higher effective stiffness.[29–32] In the first few cycles, the lower loading frequency has a relatively longer loading time and relatively smaller loading rate. Therefore, larger displacement occurs when bone-implant construct is loaded at a lower frequency during the loading and unloading phases as the bone is provided more time to deform or recover.

For a time-dependent material, the displacement increases with time when it is subjected to a constant force and recovery occurs upon force removal and again takes time. During cyclic loading, bone would only partially recover before it is subjected to the next cycle of loading. Consequently, the displacement accumulates with increasing number of cycles for all BV/TV samples and for all loading frequencies. This observation is consistent with previous experimental studies, in which the displacement of bone in a bone- implant construct was found to be a function of number of loading cycles.[13–15]

With increasing cycle numbers, the loading frequency starts playing a dominant role. When the bone-implant construct is loaded at higher frequencies, the loading/unloading time is shorter (in comparison to lower frequency loading) and the

bone is loaded again by the next cycle before it can recover from its last loading cycle. Therefore, the shift between the excitation force and displacement response occurs, which depends on the frequency of excitation. Recently, Sadeghi et al. suggested that to date, there is little data on the variation of mechanical properties of bone with increasing loading frequency.[33] Lafferty & Raju reported that for the cortical bone, with increased loading frequencies (from 30 to 125 Hz), the number of cycles required to produce fracture decreases.[22] Another indirect evidence is provided by Burr et al., who measured in vivo strains in the human tibia during walking and running, and reported that the strain experienced by bone was higher for running than walking, some of it is perhaps due to larger forces exerted during running.[34] The viscoelastic model developed from experiments on trabecular bone and employed here for a bone-implant construct is consistent with observations from previous studies. The effect of BV/TV is as expected with lower BV/TV giving higher deformations for all cycles and loading frequencies.

The aim of the current study was to develop trends – the response of interface micromotions in a bone-implant construct when it subjected to cyclic loads at different frequencies; these trends can only be evaluated by including time-dependent material models. The trends observed in this study are not only applicable to a bone-screw-like construct (e.g. locking plate[5], unilateral fixator[9], ilizarov fixator[3]) but also for joint replacement implants (e.g. total knee replacement[24]).

This study has a few limitations. We used an idealised plane strain model which implies that the implant is essentially a plate inserted in a long block of bone. These simplifications are unlikely to change the trends with respect to loading frequencies and influence of number of cycles. We show that the displacement response of bone follows a

trend with respect to BV/TV; however, we do recognise that bone microstructure has a role to play in addition to that of BV/TV as has been shown for time-independent properties.[35,36] The study assumed the bone to be isotropic, though it is accepted that it is anisotropic. [37,38] However, anisotropy is almost never included in bone-implant models as it is not straightforward to do so; isotropy which may be based on CT attenuations (which are empirically related to density or BV/TV) for subject specific models [39,40] is the common approach employed. This study suggests use of BV/TV based isotropic time-dependent viscoelastic properties rather than BV/TV based isotropic time-independent properties. As the focus of this study was to examine the time-dependent properties of trabecular bone induced accumulated deformation at the bone-implant interface with respect to different loading frequencies, the complex geometry at the implant surfact was excluded. We believe that the trends of loading frequencies related displacement at the interface remain true. Similar to several previous computational [5,9] and in vitro [13,14] studies we considered primary stability soon after the operation and before any biologically driven remodelling of bone or osseointegration occurs.

The importance of viscoelastic behaviour of bone has been discussed in several contexts – from material performance to creep deformation of bone.[41] In this study the context is implant loosening. This simple approach shows that time-dependent behaviour of bone can be incorporated readily in finite element models for the evaluation of the mechanical environment at the bone-implant interface due to cyclic loading, which commonly employed time-independent material models are not equipped to provide. It can be used to evaluate implant performance in bone of varying densities.

Acknowledgements

We gratefully acknowledge the financial support of EPSRC (Grant EP/K036939/1).

Conflict of interest

The authors declare that there is no conflict of interest.

References

1. Freeman M, Plante-Bordeneuve P. Early migration and late aseptic failure of proximal femoral prostheses. *J Bone Joint Surg Br* 2018; 76-B: 432–438.

2. Grewal R, Rimmer MG, Freeman MAR. Early migration of prostheses related to long-term surviorship. *Bone Jt Surg* 1992; 74-B: 239–242.

3. Donaldson FE, Pankaj P, Simpson AHRW. Investigation of factors affecting loosening of ilizarov ring-wire external fixator systems at the bone-wire interface. *J Orthop Res* 2012; 30: 726–732.

4. MacLeod AR, Simpson AHRW, Pankaj P. Reasons why dynamic compression plates are inferior to locking plates in osteoporotic bone: a finite element explanation. *Comput Methods Biomech Biomed Engin* 2015; 18: 1818–1825.

5. MacLeod AR, Simpson AHRW, Pankaj P. Age-related optimization of screw placement for reduced loosening risk in locked plating. *J Orthop Res* 2016; 34: 1856–1864.

6. Sundfeldt M, V Carlsson L, B Johansson C, et al. Aseptic loosening, not only a question of wear: A review of different theories. *Acta Orthop* 2006; 77: 177–197.

7. Sakaguchi RL, Borgersen SE. Nonlinear finite element contact analysis of dental implant components. *Int J Oral Maxillofac Implants* 1993; 8: 655–661.

8. Clifford RP, Lyons TJ, Webb JK. Complications of external fixation of open fractures of the tibia. *Injury* 1987; 18: 174–176.

9. Donaldson FE, Pankaj P, Simpson AHRW. Bone properties affect loosening of half-pin external fixators at the pin-bone interface. *Injury* 2012; 43: 1764–1770.

10. Huiskes R, Chao EYS, Crippen TE. Parametric analyses of pin-bone stresses in external fracture fixation devices. *J Orthop Res* 1985; 3: 341–349.

11. Taylor M, Tanner KE. Fatigue failure of cancellous bone: a possible cause of implant migration and loosening. *J Bone Joint Surg Br* 1997; 79-B: 181–182.

12. Britton JR, Lyons CG, Prendergast PJ. Measurement of the relative motion between an implant and bone under cyclic loading. *Strain* 2004; 40: 193–202.

13. Basler SE, Traxler J, Müller R, et al. Peri-implant bone microstructure determines dynamic implant cut-out. *Med Eng Phys* 2013; 35: 1442–1449.

14. Bianco R-J, Aubin C-E, Mac-Thiong J-M, et al. Pedicle screw fixation under nonaxial loads: A cadaveric study. *Spine (Phila Pa 1976)* 2016; 41: 124–130.

15. Schüller M, Drobetz H, Redl H, et al. Analysis of the fatigue behaviour characterized by stiffness and permanent deformation for different distal volar radius compression plates. *Mater Sci Eng C* 2009; 29: 2471–2477.

16. Xie S, Manda K, Wallace RJ, et al. Time Dependent Behaviour of Trabecular Bone at Multiple Load Levels. *Ann Biomed Eng* 2017; 45: 1219–1226.

17. Manda K, Wallace RJ, Xie S, et al. Nonlinear viscoelastic characterization of bovine trabecular bone. *Biomech Model Mechanobiol* 2016; 16: 173–189.

18. Manda K, Xie S, Wallace RJ, et al. Linear viscoelasticity - bone volume fraction relationships of bovine trabecular bone. *Biomech Model Mechanobiol* 2016; 15: 1631–1640.

19. Bowman SM, Guo XE, Cheng DW, et al. Creep contributes to the fatigue behavior of bovine trabecular bone. *J Biomech Eng* 1998; 120: 647–654.

20. Moore TLA, O'Brien FJ, Gibson LJ. Creep does not contribute to fatigue in bovine trabecular bone. *J Biomech Eng* 2004; 126: 321–329.

21. Haddock SM, Yeh OC, Mummaneni P V., et al. Similarity in the fatigue behavior of trabecular bone across site and species. *J Biomech* 2004; 37: 181–187.

22. Lafferty J, Raju PV V. The Influence of Stress Frequency on the Fatigue Strength of Cortical Bone. *J Biomech Eng* 1979; 101: 112–113.

23. MacLeod AR, Pankaj P, Simpson AHRW. Does screw-bone interface modelling matter in finite element analyses? *J Biomech* 2012; 45: 1712–1716.

24. Conlisk N, Howie CR, Pankaj P. Quantification of interfacial motions following primary and revision total knee arthroplasty: A verification study versus experimental data. *J Orthop Res* 2017; 1–10.

25. Keyak JH. Improved prediction of proximal femoral fracture load using nonlinear finite element models. *Med Eng Phys* 2001; 23: 165–173.

26. Shultz TR, Blaha JD, Gruen TA, et al. Cortical bone viscoelasticity and fixation strength of press-fit femoral stems: a finite element model. *J Biomech Eng* 2006; 128: 7–12.

27. Xie S, Manda K, Pankaj P. Time-dependent behaviour of bone accentuates loosening in the fixation of fractures using bone-screw systems. *Bone Joint Res* 2018; 7: 580–586.

28. Abdel-Wahab AA, Alam K, Silberschmidt V V. Analysis of anisotropic viscoelastoplastic properties of cortical bone tissues. *J Mech Behav Biomed Mater* 2011; 4: 807–820.

29. Schaffler MB, Radin EL, Burr DB. Mechanical and morphological effects of strain rate on fatigue of compact bone. *Bone* 1989; 10: 207–214.

30. Linde F, Norgaard P, Hvid I, et al. Mechanical properties of trabecular bone. Dependency on strain rate. *J Biomech* 1991; 24: 803–809.

31. Hansen U, Zioupos P, Simpson R, et al. The effect of strain rate on the mechanical properties of human cortical bone. *J Biomech Eng* 2008; 130: 1–8.

32. Wallace RJ, Pankaj P, Simpson AHRW. The effect of strain rate on the failure stress and toughness of bone of different mineral densities. *J Biomech* 2013; 46: 2283–2287.

33. Sadeghi H, Espino DM, Shepherd DET. Fatigue strength of bovine articular cartilage-on-bone under three-point bending: the effect of loading frequency. *BMC Musculoskelet Disord* 2017; 18:142: 1–8.

34. Burr DB, Milgrom C, Fyhrie D, et al. In vivo measurement of human tibial strains during vigorous activity. *Bone* 1996; 18: 405–410.

35. Zysset PK. A review of morphology-elasticity relationships in human trabecular bone: Theories and experiments. *J Biomech* 2003; 36: 1469–1485.

36. Steiner JA, Ferguson SJ, van Lenthe GH. Computational analysis of primary implant stability in trabecular bone. *J Biomech* 2015; 48: 807–815.

37. Levrero-Florencio F, Margetts L, Sales E, et al. Evaluating the macroscopic yield behaviour of trabecular bone using a nonlinear homogenisation approach. *J Mech Behav Biomed Mater* 2016; 61: 384–396.

38. Pankaj P, Xie S. The risk of loosening of extramedullary fracture fixation devices. *Injury* 2019; 50: S66–S72.

39. Goffin JM, Pankaj P, Simpson AHRW, et al. Does bone compaction around the helical bladeof a proximal femoral nail anti-rotation (PFNA) decrease the riskof cut-out?: A subject-specific computational study. *Bone Jt Res* 2013; 2: 79–83.

40. Taddei F, Schileo E, Helgason B, et al. The material mapping strategy influences the accuracy of CT-based finite element models of bones: An evaluation against experimental measurements. *Med Eng Phys* 2007; 29: 973–979.

41. Lakes R. Viscoelastic Properties of Cortical Bone. In: *Bone mechanics handbook*. CRC Press, 2001.

List of Figures

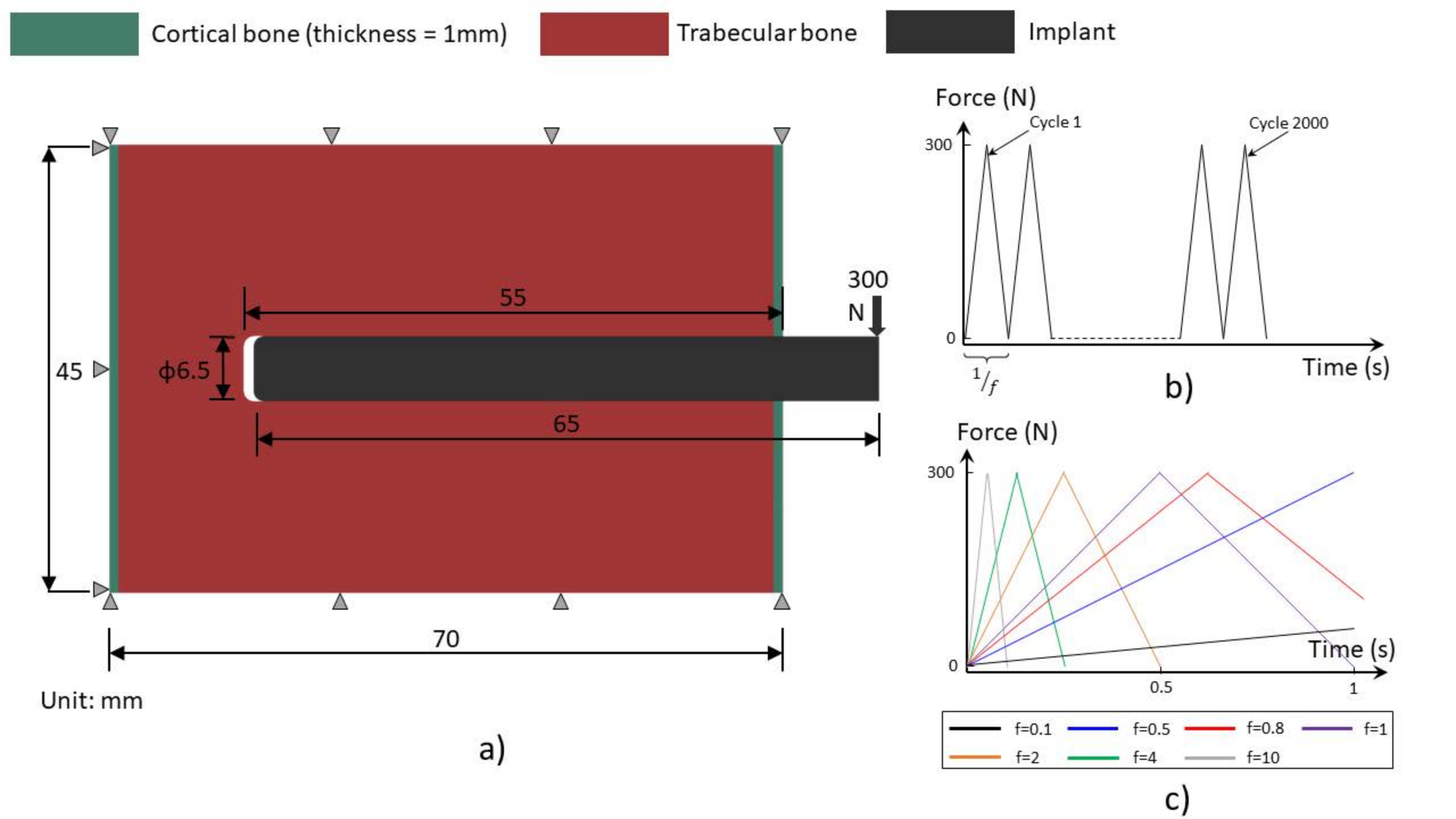
Cortical bone (thickness = 1mm)
Trabecular bone
Implant
55
300
N
45
ϕ6.5
65
70
Unit: mm
a)
Force (N)
Cycle 1
Cycle 2000
300
0
1/f
Time (s)
b)
Force (N)
300
0
Time (s)
0.5
1
f=0.1
f=0.5
f=0.8
f=1
f=2
f=4
f=10
c)

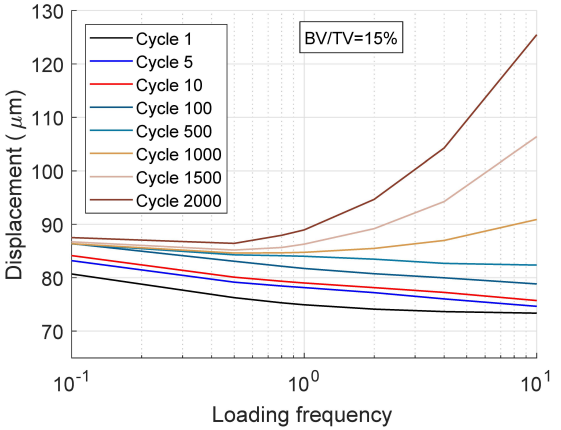
Cycle 1
Cycle 5
Cycle 10
Cycle 100
Cycle 500
Cycle 1000
Cycle 1500
Cycle 2000
BV/TV=15%
Displacement (μm)
Loading frequency

(a)

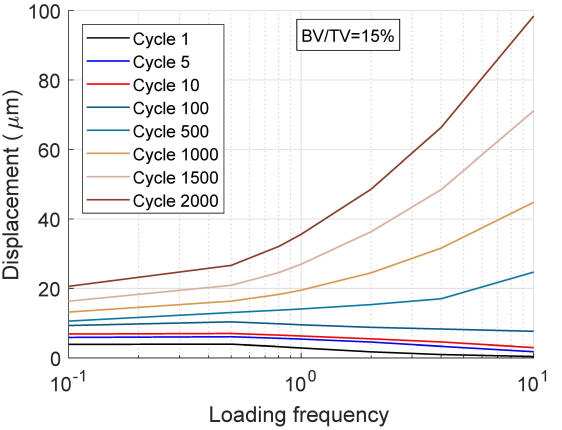
Cycle 1
Cycle 5
Cycle 10
Cycle 100
Cycle 500
Cycle 1000
Cycle 1500
Cycle 2000
BV/TV=15%
Displacement (μm)
Loading frequency

(b)

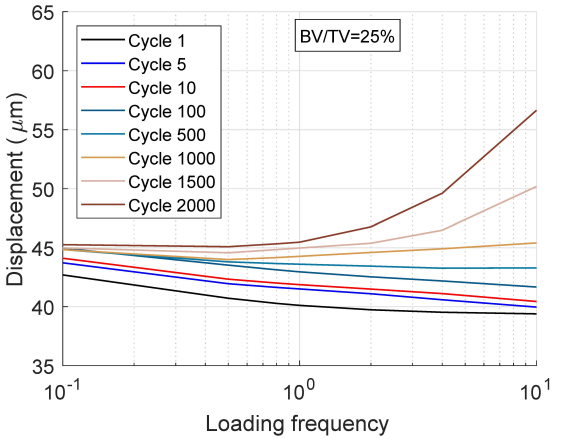
Cycle 1
Cycle 5
Cycle 10
Cycle 100
Cycle 500
Cycle 1000
Cycle 1500
Cycle 2000
BV/TV=25%
Displacement (μm)
Loading frequency

(c)

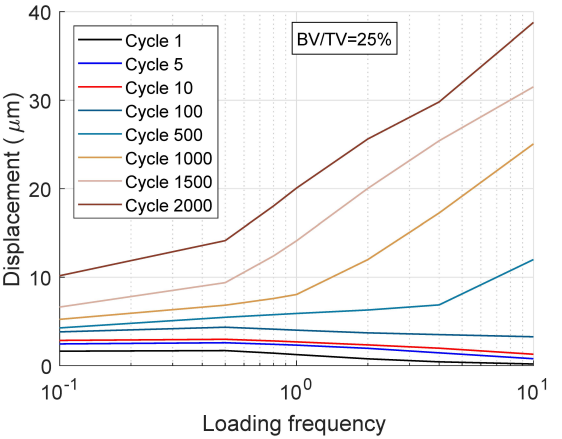
Cycle 1
Cycle 5
Cycle 10
Cycle 100
Cycle 500
Cycle 1000
Cycle 1500
Cycle 2000
BV/TV=25%
Displacement (μm)
Loading frequency

(d)

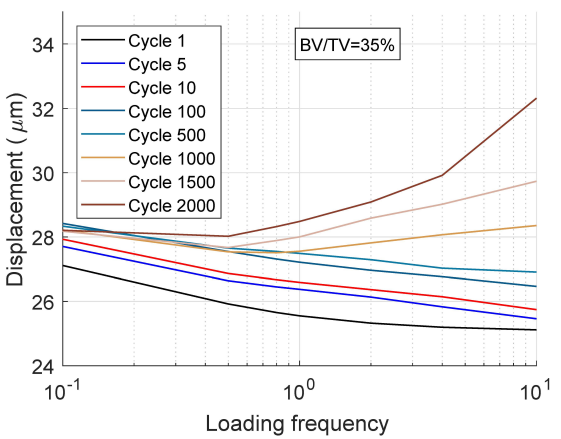
Cycle 1
Cycle 5
Cycle 10
Cycle 100
Cycle 500
Cycle 1000
Cycle 1500
Cycle 2000
BV/TV=35%
Displacement (μm)
Loading frequency

(e)

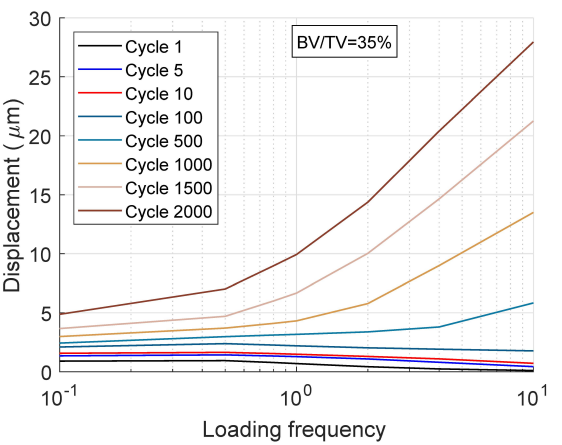
Cycle 1
Cycle 5
Cycle 10
Cycle 100
Cycle 500
Cycle 1000
Cycle 1500
Cycle 2000
BV/TV=35%
Displacement (μm)
Loading frequency

(f)

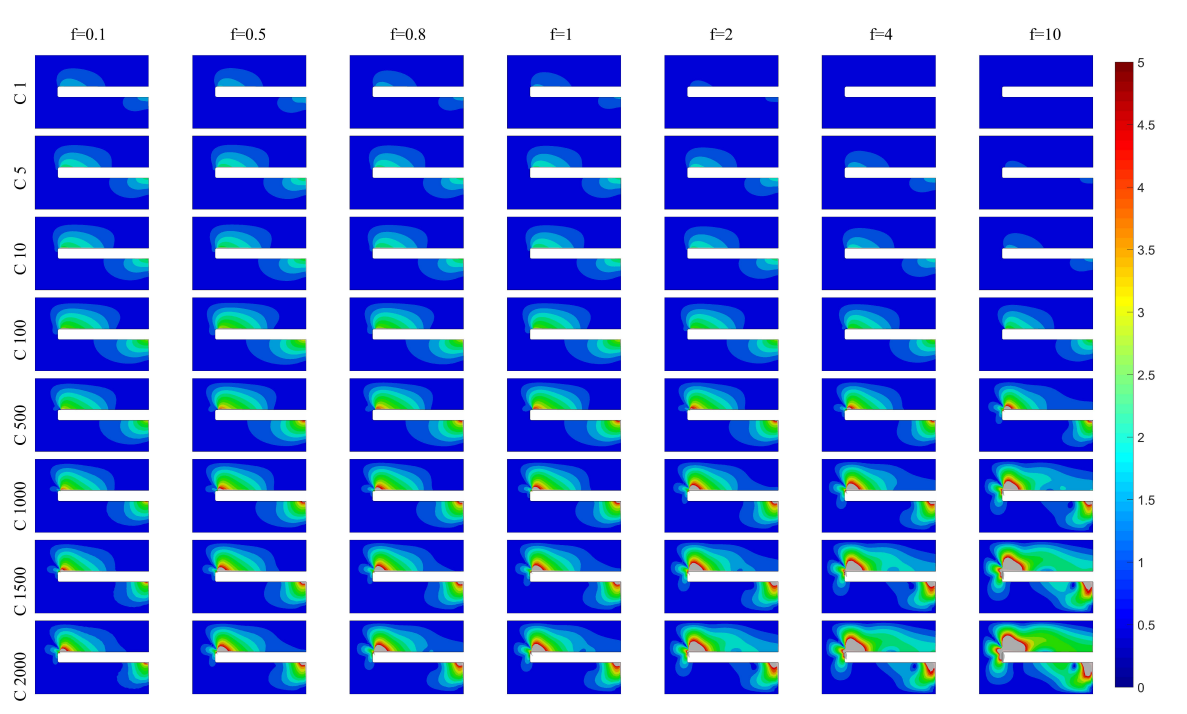
f=0.1
f=0.5
f=0.8
f=1
f=2
f=4
f=10
C 1
C 5
C 10
C 100
C 500
C 1000
C 1500
C 2000
5
4.5
4
3.5
3
2.5
2
1.5
1
0.5
0

Table 1 BV/TV-based linear viscoelastic properties for trabecular bone

Parameters	Unit	ϕ = 0.15	ϕ = 0.25	ϕ = 0.35
$E_e = B\phi^p$	MPa	139.72	287.71	463.00
$E_1 = B\widetilde{E_1}\,\phi^{p_t}$		8.36	14.03	19.73
$E_2 = B\widetilde{E_2}\,\phi^{p_t}$		14.62	24.55	34.53
$E_3 = B\widetilde{E_3}\,\phi^{p_t}$		11.63	19.54	27.48
$\rho_1 = \tilde{\rho}_1$	s		8.83	
$\rho_2 = \tilde{\rho}_2$			0.93	
$\rho_3 = \tilde{\rho}_3$			133.23	

where: B = 2043.0, p = 1.414, p^t = 1.014, $\widetilde{E_1}$ = 0.028, $\widetilde{E_2}$ = 0.049, $\widetilde{E_3}$ = 0.039, $\tilde{\rho}_1$ = 8.83, $\tilde{\rho}_1$ = 0.93, $\tilde{\rho}_3$ = 133.23